

Deep EHR Spotlight: a Framework and Mechanism to Highlight Events in Electronic Health Records for Explainable Predictions

Thanh Nguyen-Duc, MSc^{1,2}; Natasha Mulligan, MSc¹; Gurdeep S. Mannu, MBBS, MRCSEd, DPhil³; Joao H. Bettencourt-Silva, MSc, PhD¹

¹IBM Research Europe, Dublin, Ireland; ²Monash University, Melbourne, Australia;

³Nuffield Department of Population Health, University of Oxford, Oxford, UK

Abstract

The wide adoption of Electronic Health Records (EHR) has resulted in large amounts of clinical data becoming available, which promises to support service delivery and advance clinical and informatics research. Deep learning techniques have demonstrated performance in predictive analytic tasks using EHRs yet they typically lack model result transparency or explainability functionalities and require cumbersome pre-processing tasks. Moreover, EHRs contain heterogeneous and multi-modal data points such as text, numbers and time series which further hinder visualisation and interpretability. This paper proposes a deep learning framework to: 1) encode patient pathways from EHRs into images, 2) highlight important events within pathway images, and 3) enable more complex predictions with additional intelligibility. The proposed method relies on a deep attention mechanism for visualisation of the predictions and allows predicting multiple sequential outcomes.

1 Introduction

Electronic health records (EHR) are essential in supporting healthcare practitioners track their patients and deliver services. Details from patients' encounters are routinely collected in EHRs and, despite advances in machine learning and statistical modeling, these data are heterogeneous and difficult to reuse. The expectation is that routinely collected data together with deep learning techniques may help drive personalised medicine and improve the quality of health-care service delivery. Typical analytic tasks include disease classification or prediction of clinical events and a number of different deep learning architectures has been identified¹.

Most analytic architectures rely on EHR data which has undergone substantial pre-processing steps to transform or model these data before it is later ingested for analysis.

EHR data has been previously modeled as pathways² describing patient trajectories through time, and studies have also combined multi-modal information (e.g. static demographic variables with patient vitals and text notes) for prediction tasks with some degree of explainability³. Other studies have represented EHR information as a matrix of ICD9 codes versus number of visits, and used convolutional neural networks (CNNs) for prediction³.

The way in which data is modeled and represented can help support both the prediction of clinical events and the interpretability of the results, the latter being particularly important in healthcare. Bringing models into real-world use requires understanding the mechanisms by which models operate and this level of transparency is currently challenging to achieve¹. Attention mechanisms are a common way to provide visual explanations for natural images in neural networks by highlighting the most relevant events in terms of contributions to model prediction or classification. Attention mechanisms can be divided into *soft* attention and *hard* attention and their associated weights represent the degree in which the model is paying attention to certain regions of an image. While *soft* attention uses differentiable functions to produce attention weights, *hard* attention involves non-differentiable functions to generate binary weights. For example, Xu et al. exploited *soft* attention for natural image captioning⁴ and several improvements have been made to *hard* attention for the model to be differentiable (e.g. REINFORCE⁵).

In this paper we propose to represent EHR data as an image-like 2D matrix in order to predict a sequence of clinical events while providing some level of interpretation of the results. We extract features from EHRs using CNN techniques and predict sequences of clinical events using a Recurrent Neural Network (RNN) and attention techniques. RNNs are a well-known method for predicting sequential data. However, they do not perform well in practice, especially because of the vanishing gradient and long-term dependency problems⁶. Long short-term memory (LSTM)⁷ is a special kind of recurrent neural network that aims to overcome these drawbacks. LSTM consists of different gates (such as input,

output and forget gate) that allow it to learn to preserve important information and discard other information in order to effectively predict long sequences. However, vanilla LSTM does not consider the previously predicted output from a previous state in order to improve the prediction of current state. A teacher enforcing technique may be used to improve performance by keeping constraints between outputs (i.e. passing the previous prediction to the current state). LSTMs using teacher enforcing have been successfully applied to images and used in natural language processing such as image captioning⁴, as well as in sequence to sequence problems⁸.

Previous work encoding patient EHR information using autoencoders, RNNs and attention have been applied to improve model accuracy but have not relied on a combination of 2D representation while exposing attention as a mechanism to visualize important areas within a patient’s EHR^{3,9–11}.

This paper proposes *Deep EHR Spotlight*, a framework for predicting and highlighting important clinical events from pathways based on electronic health records. In particular, this paper introduces:

- a 2D pathway representation which can be used with two dimensional CNN techniques to improve visual interpretation
- a novel deep spotlight model which can highlight important events to help interpret the model’s predictions, which may include sequential events, using attention, LSTM with teacher enforcing.

Experiments were conducted on a real world dataset MIMIC-III¹² and an evaluation was carried out based on performance metrics and a domain expert review.

2 Methods

This section describes the proposed framework in detail over two parts as illustrated in Fig. 1: a) EHR Data Transformation and b) the Deep Spotlight Model. The first part is an EHR data transformation module which transforms the heterogeneous raw data from an EHR dataset into image-like representations named pathway images x with associated height and width denoted by $h \times w$, respectively. We also propose a Deep Spotlight Model, described in detail in section 2.2, which uses an attention mechanism that takes as input a pathway, x , to predict a sequence of targets (e.g., a sequence of conditions or diseases) $\tilde{y} = \{\tilde{y}_1, \tilde{y}_2, \dots, \tilde{y}_L\}$, $\tilde{y}_i \in \mathbb{R}^K$, where K is the number of possible events to classify at \tilde{y}_i and L is the maximum length of the sequence). The attention mask produced can highlight (‘spotlight’) the important events that significantly contribute to the model’s decision using an attention mechanism described in section 2.2.2. Each prediction \tilde{y}_i corresponds to specific highlighted events in the pathway, described in section 2.1.

The Pathway Composition module takes the heterogeneous EHR data to produce pathway images consisting of transformed EHR data in a 2-D image-like representation (defined in Section 2.1). The pathway image x inputs to the Deep Spotlight model to predict a sequence of targets \tilde{y} that are pushed closer to the ground truth $y = \{y_1, y_2, \dots, y_L\}$, $y_i \in \mathbb{R}^K$ (i.e. the labelled data used for training) by minimizing cross-entropy loss and its attention masks corresponding to each prediction \tilde{y}_i . The model and approach are described in detail in the next sections.

2.1 Pathway Data Representation

Let \mathbb{D} represent a data model consisting of medical codes, where the i -th entry has code $m_i \in \mathbb{M}$ where $1 \leq i \leq N$ in a total of N possible codes. Codes may be extracted and mapped directly to terminologies such as ICD or LOINC and each code has an associated dimension, h_1, \dots, h_6 , of six pre-defined dimensions that group events of similar nature together (e.g. procedures, observations and medications) as shown in Figure 2.

A pathway describes a patient’s hospital admission as a series of events $E = (r, t, m, h)$ where:

- r is the patient identifier.
- t is the sequence in which events occurred, which can be calculated using the time in days since the day of primary diagnosis for an admission recorded for patient r . Events without an associated time have $t = 0$.

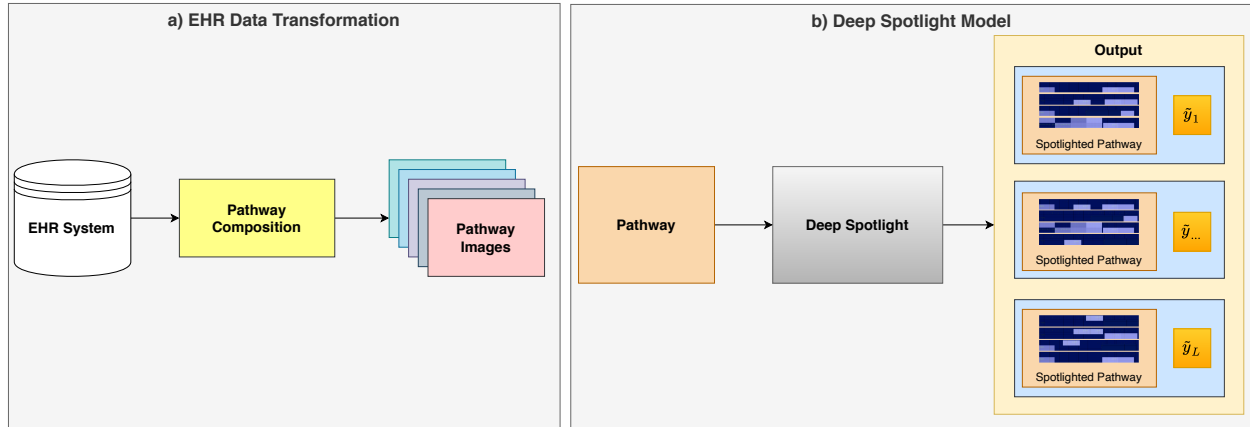


Figure 1: Overview of the framework and its two parts: a) EHR Data Transformation used to compose pathways and b) Deep Spotlight Model used to predicting a sequence of events y and highlight areas that explain predictions \hat{y}_i .

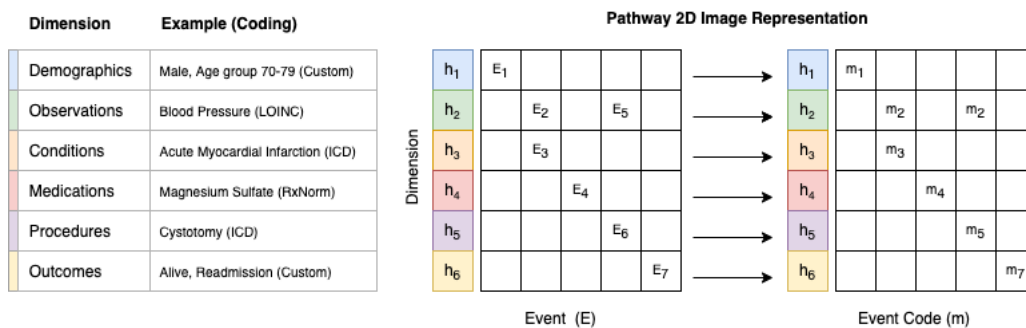


Figure 2: 2D-image representation for a given pathway. The y-axis represents the pre-defined dimensions h and the x-axis the pathway events from which codes and values are used.

- $m \in \mathbb{M}$ is an event code, such as a specific ICD9, LOINC code, or other, as described in Figure 2.
- h is the dimension associated with medical code m as described in Figure 2.

Thus, a pathway for a patient r is defined as an ordered set of events $\mathbb{P} = \{E_1, E_2, \dots, E_M\}$ where:

1. E_i is of the form (r, t_i, m_i, h_i) for $1 \leq i \leq M$,
2. $t_i \leq t_{i+1}$ for $1 \leq i \leq M$,
3. M is total number of events in a pathway.

Subsequently, a pathway x can be described as a 2-D image by arranging dimensions h across the y-axis and events E across the x-axis as illustrated in Figure 2. For each event in the pathway image x , the code m_i may be concatenated, resulting in a single value equivalent to each pixel in an image. This representation enables a spatial correlation for feature extraction using two dimensional CNN techniques (e.g., medications and procedures in Fig. 2) and may provide better visualization in practice. The above pathway model is inspired by previous work² and may be remodelled to include, for example, the values associated with each event code m .

2.2 Deep Spotlight Model

Deep Spotlight model is designed to predict a sequence of output events and to highlight input events which contribute to the prediction. We denote the three main modules: feature extractor f , attention module s and long short-term

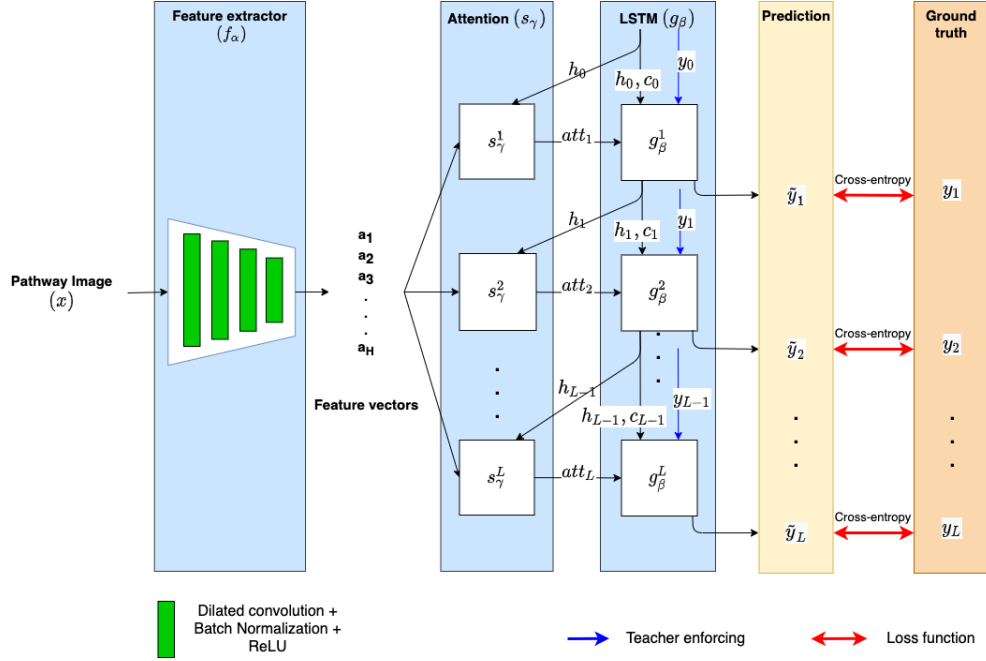
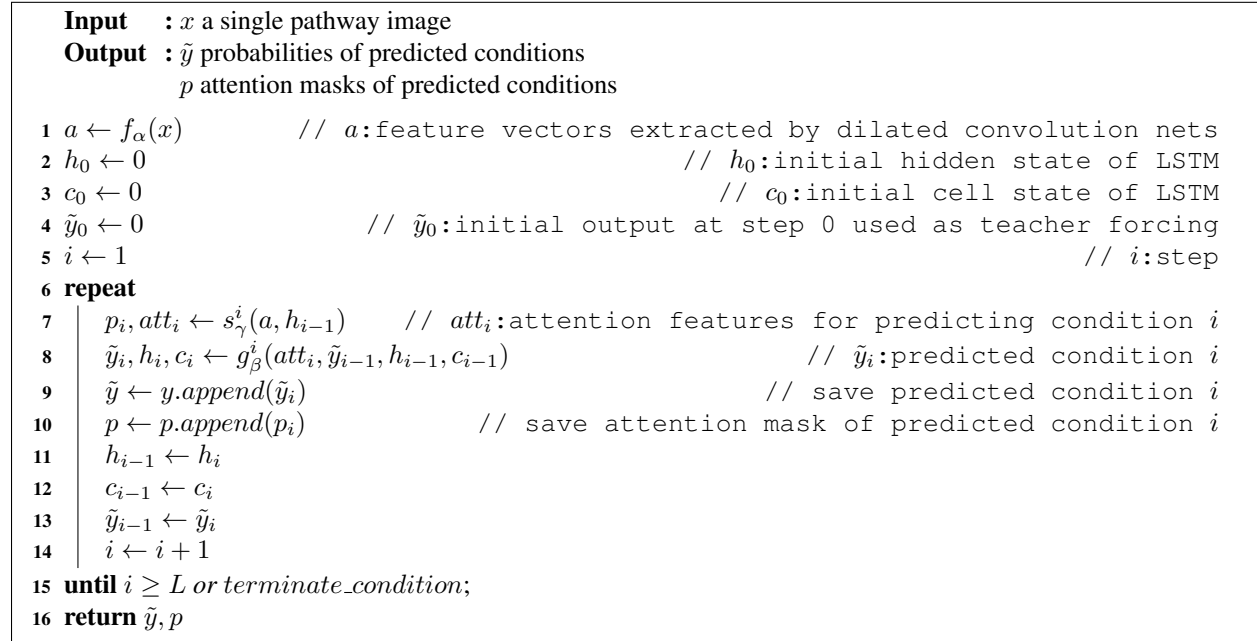


Figure 3: Training process of proposed deep spotlight model consisting of encoder f , attention module s and LSTM g parameterized by α , γ and β respectively. The prediction \tilde{y} is pushed close to ground truth y by minimizing cross-entropy loss and current prediction \tilde{y}_i is also enforced during training process by label y_{i-1} called teacher enforcing¹³.



Algorithm 1: Predicting process of a sequence of medical events \tilde{y} and attention masks p corresponding to each \tilde{y}_i given an input pathway image x .

memory module g which are parameterized by α , γ and β respectively. The feature extractor uses convolutional neural networks f_α (CNN) to extract features a from input pathway image. The attention module s_γ produces attention masks p with values from $[0; 1]$ in order to highlight important events that significantly contributed to the predictions. This

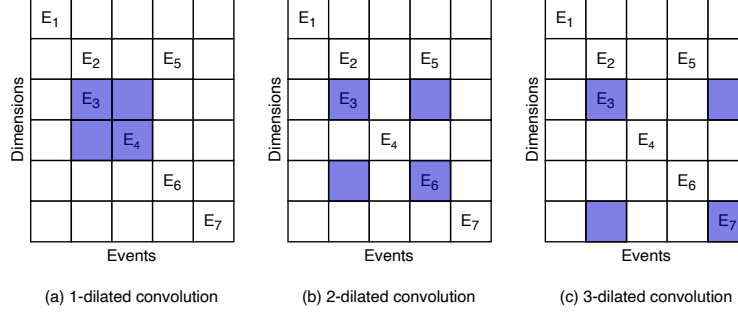


Figure 4: Receptive field expansion of a 2×2 convolution filter at different dilation factors on pathway image.

is done by increasing the weights for important feature regions of a and decreasing for unimportant ones. The LSTM module is used to generate the predicted sequence targets \tilde{y} by taking the output of the attention module, as shown in Fig 3.

Note that we take the dimension (row) from the pathway image which contains a sequence of events that represents our training ground-truth y . Therefore, the input image size is $h - 1 \times w$. For example, in order to predict conditions, the condition dimension in Fig. 2 may be taken to become ground-truth y .

2.2.1 Feature extractor using dilated convolution (f_α)

Vanilla convolutional layers¹⁴ do not perform well in capturing the global context from images because small blocks of pixels can only be influenced by their filter size¹⁵, especially in sparse signals; however, using larger filter sizes requires more learnable parameters which lead to computational expensive and the *data hungry* problem. Specifically, we observed that pathways extracted from MIMIC-III are highly sparse as empty elements can be $14 \times$ more frequent than encoded events. Therefore, to overcome these drawbacks our feature extractor f_α efficiently extracts features from the input pathway image using dilated convolution layers¹⁵. The motivation for feature extractor architecture is based on the fact that the dilated convolutions support exponentially expanding receptive fields, which is the implicit area captured on the input, while the number of parameters associated with the layer are identical. In simple intuition in Fig. 4, the dilated convolution layer is just a convolution layer applied to input with defined gaps. Moreover, various well-known deep learning architectures use batch normalization¹⁶ to tackle the internal covariate shift problem in deep neural networks, and ReLU¹⁷ to avoid the vanish gradient problem during training (e.g. ResNet¹⁸, DenseNet¹⁹). Thus, our feature extractor consists of layers where each contains a dilated convolution layer, batch normalization and ReLU, as shown in Fig. 3. The output from the dilated convolution networks is a set of feature vectors a :

$$a = \{a_1, a_2, \dots, a_H\}, a_i \in \mathbb{R}^F, \quad (1)$$

where $H = h' \times w'$ is the number of flatten output feature vectors from the last convolutional layer which corresponds to spatial locations $h - 1 \times w$ of the input pathway and F is the number of convolutional filters at the last layer of f_α . By using dilated CNN, we can leverage the pathway image representation by efficiently encoding spatial correlations to feature vectors a which is the input to the attention module (see Section 2.2.2).

2.2.2 Attention mechanism (s_γ) to highlight events

In this paper, we use *soft* attention²⁰ to produce attention mask p in order to highlight important events in the pathway image that significantly contribute to the model's prediction. The attention mechanism mimics human behavior when focusing on the most informative regions to make decisions. It can also be efficiently trained using popular gradient-based methods in current deep learning frameworks. Our attention module s_γ leverages fully connected neural networks which take feature vectors a and hidden state h_{i-1} from the LSTM (defined in Section 2.2.3) as input in order to generate $score_i$ as in step i in Eq. 2.

$$score_i = s_\gamma^i(a, h_{i-1}). \quad (2)$$

The attention mask p_i , used for visualizing the highlighted areas in Fig.1, is then calculated by passing $score_i$ through the softmax function that produces attention weights from $[0;1]$, as shown in Eq. 3.

$$p_i = softmax(score_i). \quad (3)$$

Finally, attention features att_i are computed using element-wise multiplication between a and p_i to select important (spotlighted) regions.

$$att_i = a \odot p_i. \quad (4)$$

Attention mask p_i gives a score for each extracted feature vector a which corresponds to a location in the pathway image. The higher the value, the more important the events that contributed to the model’s prediction.

2.2.3 Long short-term memory network (g_β) for sequence prediction

An LSTM network is used in our framework to improve the performance of predicting sequences and has memory states, hidden state h_i , and cell state c_i at step i . Specifically, during training, the LSTM module takes the most informative extracted features (weighted attention features) att_i from the *soft* attention module’s output, previous state (h_{i-1} and c_{i-1}) and previous ground-truth y_{i-1} to predict a target (e.g., a condition or disease) \tilde{y}_i at step i and output information for next prediction (h_i and c_i). Moreover, using previous ground-truth as an input, we can improve the constrains of the LSTM with the teacher enforcing technique¹³, as shown in Fig. 3. The LSTM predicts elements one by one \tilde{y}_i in \tilde{y} at every step i until reaching terminate conditions. Note that we do not have previous ground-truth y_{i-1} during the prediction state; therefore, a new prediction \tilde{y}_i is enforced by previous prediction \tilde{y}_{i-1} that improves the predicted sequence’s accuracy, as shown in Alg. 1.

3 Results and Discussion

This section first describes the results of the transformations to compose pathway images using the MIMIC-III dataset. The performance results of the proposed Deep EHR Spotlight framework are described in section 3.2 and an evaluation with a domain expert is described in section 3.3.

3.1 Creating Pathway Images from the MIMIC-III Dataset

Pathway images were produced using the MIMIC-III dataset and based on the definitions provided in 2.1. ICD9 codes were reclassified into a smaller number of disease groups of similar codes based on a re-classification system by *Rassekh et. al.*²¹. Other approaches may be used to group ICD codes together for specific use cases, however, this was considered sufficient to train the models presented in this paper and to support building the proposed framework. Selecting a large enough amount of training data was also constrained on the length of the pathways (i.e. the x-axis where event codes are displayed). Overall 58,976 pathway images were produced across 102 different diagnosis groups and 56% of those had a length of 400 or under. The selection of diagnosis groups was based on balancing the most frequent conditions (diagnosis groups) with the lengths of the pathways in order to provide a large enough training set. Furthermore, the pathways selected also have a sequence of conditions y (based on the diagnosis codes groups) which include at most $L = 2$ conditions. Specifically, sequence y begins with one of the three selected main conditions $\{Birth\ Outcome, Cerebrovascular\ Disease, Ischemic\ Heart\ Disease\}$, and is followed by an optional second condition from the 99 remaining most frequent conditions. The second condition was also selected based on frequency, as shown in Table 1. A total of 11,400 pathway images (i.e. the first three rows in Table 1) were selected and split 80% for training and 20% for testing. The task undertaken to demonstrate the developed framework involves predicting a first main condition in a pathway followed by a second condition. For this reason the pathway image dimension h associated with conditions was removed from the training set.

Condition (Diagnosis Group)	Abbreviation	Pathways (N)	Precision	Recall	F1
Birth Outcome	BO	6675	0.999	0.996	0.997
Cerebrovascular Disease	Ce	1893	0.916	0.903	0.909
Ischemic Heart Disease	IH	2832	0.933	0.948	0.941
BO → Elective Surgery	BO-NH	616	0.623	0.494	0.551
BO → Perinatal Condition	BO-PC	3931	0.912	0.797	0.850
Ce → Arrhythmia	Ce-Ar	133	0.529	0.187	0.277
Ce → Neurological Disorder	Cr-Ne	310	0.914	0.348	0.504
IH → Cardiomyopathy & HF	IH-Ca	450	0.463	0.221	0.299
IH → Hypertension	IH-Hy	321	0.583	0.219	0.318

Table 1: Performance of the proposed framework (precision, recall and F1) for predicting a given condition or a sequence of two conditions. This table also shows the number of pathway images for each condition. The diagnoses codes used for each condition were selected based on an ICD9 re-classification system²¹.

		Predicted Condition								
		BO	BO-NH	BO-PC	Ce	Ce-Ar	Cr-Ne	IH	IH-Ca	IH-Hy
True Condition	BO	99.86	0	0	0	0	0	0.13	0	0
	BO-NH	0	62.32	26.08	0	0	0	0	0	0
	BO-PC	0	4.58	91.06	0	0	0	0	0	0
	Ce	1.40	0	0	91.54	0	0	7.041	0	0
	Ce-Ar	0	0	0	5.88	52.94	5.88	0	0	0
	Cr-Ne	0	0	0	0	5.714	91.42	0	0	0
	IH	0	0	0	6.68	0	0	93.31	0	0
	IH-Ca	0	0	0	0	0	0	4.87	46.341	14.63
	IH-Hy	0	0	0	0	0	0	0	14.70	61.76

Table 2: Confusion matrix whose vertical axis shows ground-truth conditions and horizontal axis illustrates predicted conditions (%).

3.2 Performance Evaluation

The proposed framework was first evaluated by computing performance metrics: precision, recall and F1 score, as shown in Table 1. Whilst these metrics are computed by comparing predicted \tilde{y}_0 and labeled y_0 , another metric (Intersection over union (IoU), described later) can be calculated to evaluate the predicted sequence \tilde{y} against a ground-truth (labelled) sequence y . With respect to precision and recall, the proposed method achieved adequate scores (over 90% F1 scores) for predicting the main condition alone. However, due to the small amount of data and their heterogeneity, F1 scores for the sequence of two conditions were significantly lower. For example, as seen in Table 1, there are very few training samples for *Cerebrovascular Disease* → *Arrhythmia* (133 pathways, F1 27%) and *Ischemic Heart Disease* → *Hypertension* (312 pathways, F1 31%). It is expected that the proposed method may reach better performance scores for predicting sequences of conditions with sufficiently larger amounts of training data. For example, *Birth Outcome* → *Perinatal Condition* (3931 pathways) shows an F1 score of 85%. Moreover, a confusion matrix was calculated and is shown in Table 2. The proposed approach shows good performance on *Birth Outcome*, *Cerebrovascular* and *Ischemic Heart Disease* reaching precisions 99.86%, 91.54% and 93.31%, respectively. We also observed that the performance gradually drops for *Ischemic Heart Disease* → *Cardiomyopathy* and *Ischemic Heart Disease* → *Hypertension* due to a highly imbalanced dataset.

Intersection over union (*IoU*) is a metric for evaluating the differences between predicted sequence \tilde{y} and ground-truth sequence y . *IoU* is measured by overlapping \tilde{y} and y as shown in Eq. 5

$$IoU = 2 \frac{\tilde{y} \cap y}{\tilde{y} \cup y}, \quad (5)$$

where *IoU* is equal to 1 if two sequences are perfectly matched. The calculated average *IoU* metric across all pathways

Predicted Condition	Specifically Related	Related	Not Related
Birth Outcome (BO)	14	6	0
Cerebrovascular Disease (Ce)	6	14	0
Ischemic Heart Disease (IH)	15	5	0
(BO \rightarrow) Elective Surgery	17	3	0
(BO \rightarrow) Perinatal Condition	18	2	0
(Ce \rightarrow) Arrhythmia	15	4	1
(Ce \rightarrow) Neurological Disorder	16	4	0
(IH \rightarrow) Cardiomyopathy & HF	7	12	1
(IH \rightarrow) Hypertension	8	12	0

Table 3: Evaluation of the top 20 events highlighted by the attention mask for each predicted condition where (\cdot) shows the first predicted condition.

was 0.75, showing agreement between the predicted sequence against the ground-truth.

4 Domain Expert Evaluation

The framework was further evaluated with respect to the attention mask and whether it is highlighting important events across all pathways. While the attention mask p_i values range between 0 and 1, a threshold was set at 0.9 to obtain the top 20 events highlighted by the mask in all pathways of the testing set. Several events may be highlighted in each pathway image, however, only those that contributed most significantly to the predicted condition \tilde{y}_i were selected (i.e., corresponding to the locations of threshold=0.9 in p_i). With the help of a domain expert, the top 20 events were inspected and a determination was made on whether the event codes were: specifically related to the predicted condition(s), generally related (not necessarily specific to the predicted condition), or not related, as shown in Table 3. Despite this evaluation being carried out in a small sample of the highlighted events and by a single observer, it provides reassuring results that most events highlighted as important were indeed related to the predicted condition. One of the limiting factors in this evaluation is the absence of values for the event codes. For example, a large proportion of events highlighted are LOINC codes referring to blood tests and data about the results of the blood tests was not included in our experiments. As described in section 2.1, adding values to each event code is possible, however, that would introduce additional sparseness and more training data would be required to test the developed framework. Figure 5 shows an example of a pathway image and the prediction results provided by the proposed framework as highlighted areas. Pathway image A) in Fig. 5 shows the highlighted areas that are most predictive of *Cerebrovascular* alone, and pathway image B) shows highlighted areas predicting *Cerebrovascular* \rightarrow *Neurological Disorder* for the same pathway. Fig. 5 also shows the pathway image when zoom is applied. A selected segment of the highlighted area was further expanded into text for readability and shows an example of the event codes.

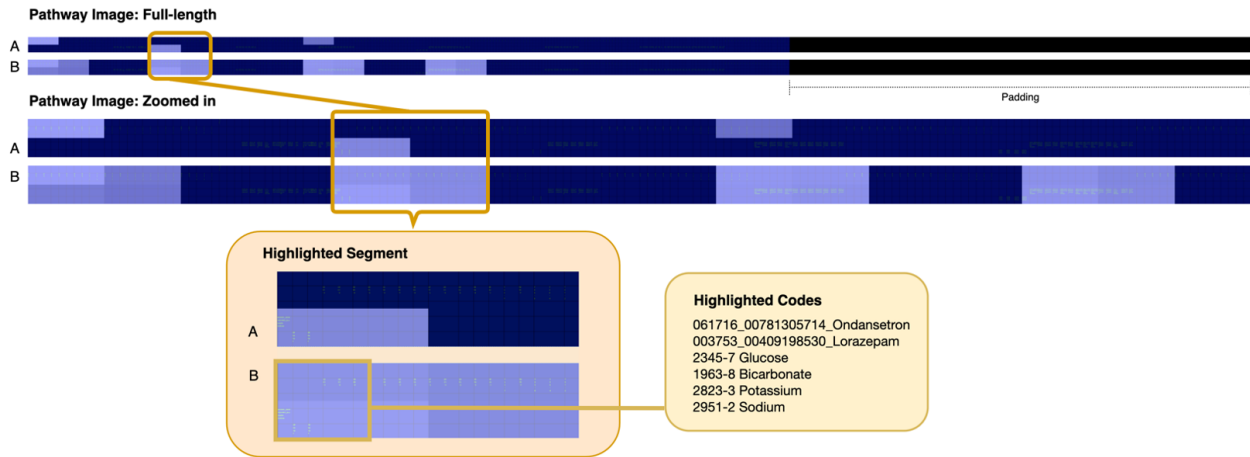


Figure 5: Example of a pathway image (output of the proposed framework) showing the highlighted areas that predicted the pathway’s conditions: Cerebrovascular disease alone (A) and Cerebrovascular disease followed by a Neurological Disorder (B). The full-length image shows a darker area denoting padding.

5 Conclusion

This paper proposes a new framework for predicting and highlighting important clinical events from electronic health records (EHRs). In particular, this paper proposes to transform EHR data into pathways and 2D pathway images, which can then be used with two dimensional CNN techniques to support visual interpretation. The proposed Deep EHR Spotlight framework can highlight regions in pathway images which are particularly important for the predictions. In this paper we used the MIMIC-III dataset, which produced highly sparse pathway images. The performance results were adequate (i.e. F1 scores > 90%) when a larger number of training data was available. The top events appearing in highlighted masks were also evaluated by a domain expert and found to be mostly related and specific to the predicted conditions. These are reassuring results that demonstrate the value in the proposed approach. However, further work is needed to substantiate these results, improve the methods for a specific use case and compare with other techniques and approaches. As future work we are planning to test the proposed framework on significantly larger datasets as well as remodeling the pathway images and their dimensions for more specific clinical use cases. This will allow predicting individual conditions and taking into account events with associated codes (e.g. haemoglobin test) and respective values (e.g. 20 g/dL). Further work is also needed to continue to evaluate the events highlighted by the attention mask for different thresholds.

References

1. C. Xiao, E. Choi, and J. Sun. Opportunities and challenges in developing deep learning models using electronic health records data: a systematic review. *Journal of the American Medical Informatics Association*, 25(10):1419–1428, 10 2018.
2. Joao H Bettencourt-Silva, Jeremy Clark, Colin S Cooper, Robert Mills, Victor J Rayward-Smith, and Beatriz de la Iglesia. Building data-driven pathways from routinely collected hospital data: A case study on prostate cancer. *JMIR Medical Informatics*, 3(3):e26, Jul 2015.
3. Q. Suo, F. Ma, Y. Yuan, M. Huai, W. Zhong, J. Gao, and A. Zhang. Deep Patient Similarity Learning for Personalized Healthcare. *IEEE Transactions on NanoBioscience*, 17(3):219–227, 07 2018.
4. Kelvin Xu, Jimmy Ba, Ryan Kiros, Kyunghyun Cho, Aaron Courville, Ruslan Salakhudinov, Rich Zemel, and Yoshua Bengio. Show, attend and tell: Neural image caption generation with visual attention. In *Proceeding of ICML*, pages 2048–2057, 2015.

5. Ronald J Williams. Simple statistical gradient-following algorithms for connectionist reinforcement learning. *Machine Learning*, 8(3-4):229–256, 1992.
6. Yoshua Bengio, Patrice Simard, and Paolo Frasconi. Learning long-term dependencies with gradient descent is difficult. *IEEE Transactions on Neural Networks*, 5(2):157–166, 1994.
7. Sepp Hochreiter and Jürgen Schmidhuber. Long short-term memory. *Neural Computation*, 9(8):1735–1780, 1997.
8. Ilya Sutskever, Oriol Vinyals, and Quoc V Le. Sequence to sequence learning with neural networks. In *Proceeding of NIPS*, pages 3104–3112, 2014.
9. Alvin Rajkomar, Eyal Oren, Kai Chen, Andrew M Dai, Nissan Hajaj, Michaela Hardt, Peter J Liu, Xiaobing Liu, Jake Marcus, Mimi Sun, et al. Scalable and accurate deep learning with electronic health records. *NPJ Digital Medicine*, 1(1):18, 2018.
10. Edward Choi, Mohammad Taha Bahadori, Jimeng Sun, Joshua Kulas, Andy Schuetz, and Walter Stewart. Retain: An interpretable predictive model for healthcare using reverse time attention mechanism. In *Proceeding of NIPS*, pages 3504–3512, 2016.
11. Qiuling Suo, Fenglong Ma, Ye Yuan, Mengdi Huai, Weida Zhong, Jing Gao, and Aidong Zhang. Deep patient similarity learning for personalized healthcare. *IEEE Transactions on NanoBioscience*, 17(3):219–227, 2018.
12. A. E. Johnson, T. J. Pollard, L. Shen, L. W. Lehman, M. Feng, M. Ghassemi, B. Moody, P. Szolovits, L. A. Celi, and R. G. Mark. MIMIC-III, a freely accessible critical care database. *Scientific Data*, 3:160035, May 2016.
13. Ronald J Williams and David Zipser. A learning algorithm for continually running fully recurrent neural networks. *Neural Computation*, 1(2):270–280, 1989.
14. Yann LeCun, Léon Bottou, Yoshua Bengio, and Patrick Haffner. Gradient-based learning applied to document recognition. *Proceedings of the IEEE*, 86(11):2278–2324, 1998.
15. Fisher Yu and Vladlen Koltun. Multi-scale context aggregation by dilated convolutions. *arXiv preprint arXiv:1511.07122*, 2015.
16. Sergey Ioffe and Christian Szegedy. Batch normalization: Accelerating deep network training by reducing internal covariate shift. *arXiv preprint arXiv:1502.03167*, 2015.
17. Vinod Nair and Geoffrey E Hinton. Rectified linear units improve restricted boltzmann machines. In *Proceeding of ICML*, 2010.
18. Kaiming He, Xiangyu Zhang, Shaoqing Ren, and Jian Sun. Deep residual learning for image recognition. In *Proceedings of CVPR*, pages 770–778, 2016.
19. Gao Huang, Zhuang Liu, Laurens Van Der Maaten, and Kilian Q Weinberger. Densely connected convolutional networks. In *Proceedings of CVPR*, pages 4700–4708, 2017.
20. Dzmitry Bahdanau, Kyunghyun Cho, and Yoshua Bengio. Neural machine translation by jointly learning to align and translate. In *Proceeding of ICLR*, 2015.
21. S. R. Rassekh, M. Lorenzi, L. Lee, S. Devji, M. McBride, and K. Goddard. Reclassification of ICD-9 Codes into Meaningful Categories for Oncology Survivorship Research. *Cancer Epidemiol*, 2010:569517, 2010.